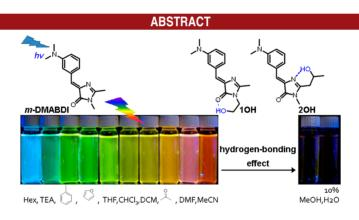
## Site-Selective Hydrogen-Bonding-Induced **Fluorescence Quenching of Highly** Solvatofluorochromic GFP-like **Chromophores**

Guan-Jhih Huang,<sup>†</sup> Jinn-Hsuan Ho,<sup>‡</sup> Ch. Prabhakar,<sup>†</sup> Yi-Hung Liu,<sup>†</sup> Shie-Ming Peng,<sup>†</sup> and Jye-Shane Yang\*,<sup>†</sup>

Department of Chemistry, National Taiwan University, Taipei, Taiwan, 10617, and Department of Chemical Engineering, National Taiwan University of Science and Technology, Taipei, Taiwan, 10607

jsvang@ntu.edu.tw

## Received August 12, 2012



The unconstrained green fluorescence protein (GFP)-like chromophore m-DMABDI displays a high solvatofluorochromicity in aprotic solvents, but the fluorescence is guenched in protic solvents. According to the site-specific intramolecularly hydrogen-bonded analogs 10H and 20H, the hydrogen bonding to the carbonyl oxygen is more important than that to the imino nitrogen of the imidazolinone group in the fluorescence quenching.

Hydrogen bonding is a directional noncovalent interaction that plays an important role in the structures and properties of numerous natural and artificial molecules, supermolecules,

(3) (a) Hermant, R. M.; Bakker, N. A. C.; Scherer, T.; Krijnen, B.; Verhoeven, J. W. J. Am. Chem. Soc. 1990, 112, 1214-1221. (b) Lewis, F. D.; Yoon, B. A.; Arai, T.; Iwasaki, T.; Tokumaru, K. J. Am. Chem. Soc. 1995, 117, 3029-3036.

and polymers.<sup>1-7</sup> Hydrogen-bonding interactions in the excited state might lead to fluorescence quenching due to rapid internal conversion or proton/electron transfer.<sup>2-7</sup> However, the phenomenon of H-bonding-induced fluorescence quenching is barely predictable for a new chromophore, as the fluorescence-quenching mode is sensitive to substrate conformation<sup>4</sup> and H-bonding location<sup>5</sup> and/or orientation.<sup>6</sup> For a chromophore containing more than one H-bonding site,<sup>7</sup> experimental identification of the site responsible for the fluorescence quenching is fundamentally

ORGANIC LETTERS

2012 Vol. 14, No. 19

5034-5037

<sup>&</sup>lt;sup>†</sup>National Taiwan University.

 <sup>\*</sup>National Taiwan University of Science and Technology.
 (1) (a) Hu, W.; Zhu, N.; Tang, W.; Zhao, D. Org. Lett. 2008, 10, 2669–2672. (b) Hariharan, M.; Siegmund, K.; Lewis, F. D. J. Org. Chem. 2010, 75, 6236–6243. (c) Li, X.; Fang, Y.; Deng, P.; Hu, J.; Li, T.; Feng, W.; Yuan, L. Org. Lett. 2011, 13, 4628–4631. (d) Gonzalez-Rodriguez, D.; Schenning, A. P. H. J. Chem. Mater. 2011, 23, 310-325. (e) Such, G. K.; Johnston, A. P. R.; Caruso, F. Chem. Soc. Rev. 2011, 40, 19-29.

<sup>(2) (</sup>a) Zimmer, M. Chem. Rev. 2002, 102, 759-781. (b) Waluk, J. Acc. Chem. Res. 2003, 36, 832-838. (c) Zhao, G.-J.; Han, K.-L. Acc. Chem. Res. 2012, 45, 404-413.

<sup>(4)</sup> Petkova, I.; Mudadu, M. S.; Singh, A.; Thummel, R. P.; van Stokkum, I. H. M.; Buma, W. J.; Waluk, J. J. Phys. Chem. A 2007, 111, 11400-11409.

<sup>(5)</sup> Morimoito, A.; Yatsuhashi, T.; Shimada, T.; Biczók, L.; Tryk, D. A.; Inoue, H. J. Phys. Chem. A 2001, 105, 10488-10496.

<sup>(6) (</sup>a) Sugitha, M.; Shimada, T.; Tachibana, H.; Inoue, H. Phys. Chem. Chem. Phys. 2001, 3, 2012-2017. (b) Morimoto, A.; Yatsuhashi, T.; Shimada, T.; Kumazaki, S.; Yoshihara, K.; Inoue, H. J. Phys. Chem. A 2001, 105, 8840-8849.

<sup>(7)</sup> Zhao, G.-J.; Liu, J.-Y.; Zhou, L.-C.; Han, K.-L. J. Phys. Chem. B 2007, 111, 8940-8945.

important but is rarely demonstrated. We report herein one such example with the modified green fluorescent protein (GFP) chromophores *meta*-dimethylaminobenzylidenedimethylimidazolinone (*m*-DMABDI), **10H**, and **20H** (the *m*-DMABDIs).

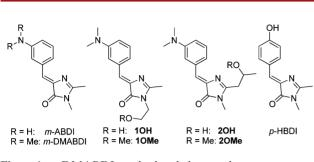
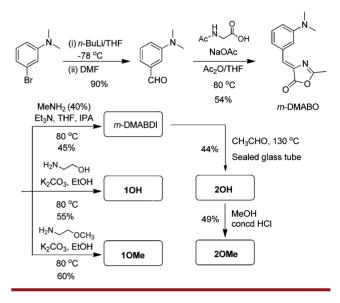


Figure 1. *m*-DMABDIs and related chromophores.

Molecular design of the *m*-DMABDIs is based on our previous observation of drastic fluorescence quenching of m-ABDI on going from aprotic to protic solvents (e.g., fluorescence quantum yield  $\Phi_{\rm f} = 0.34$  in hexane and <0.001 in MeOH), which indicates the presence of H-bonding-induced excited-state deactivation.<sup>8</sup> This differs from the extremely weak ( $\Phi_{\rm f} < 0.001$ ) and solvent-independent fluorescence properties of the parent GFP chromophore, para-hydroxybenzylidenedimethylimidazolinone (p-HBDI), revealing a significant meta-amino substituent effect.9 The H-bonding modes associated with the imidazolinone group in m-ABDI should be important, as the photoinduced internal charge transfer increases the charge density of this group. The presence of two H-bond acceptors, the carbonyl oxygen and the imino nitrogen, in the imidazolinone group provides a unique opportunity for investigating their relative contribution to the observed fluorescence quenching. To avoid the complication of H-bonding interactions between the amino group (H-bond donor) in m-ABDI and polar aprotic solvents (e.g., the nitrogen of MeCN), the dimethylamino analog *m*-DMABDI and the site-specific intramolecularly H-bonded derivatives 10H and 20H were designed. The intramolecular H-bond is in a seven-membered ring in 10H but in a six-membered ring in 20H. On the basis of DFT (B3LYP/6-31G\*\*) calculations, the optimized structures of 10H and 20H (Figure S1) exhibit the expected intramolecular H-bond and are favorable by 2.49 and 5.72 kcal  $mol^{-1}$ . respectively, relative to non-H-bonded conformations (Tables S1 and S2). With the corresponding non-H-bonded systems 10Me and 20Me as reference compounds, the carbonyl vs imino H-bonding effect on the fluorescence quenching can be addressed.

The *m*-DMABDIs were prepared according to a modified version of Niwa's synthetic protocol (Scheme 1).<sup>10</sup> The chromophores *m*-DMABDI, **10H**, and **10Me** were obtained from the common intermediate *m*-DMABO by reacting with the corresponding aliphatic amines. The OH-containing side chain in **20H** was introduced from the reaction of *m*-DMABDI and acetaldehyde.<sup>11</sup> Acetaldehyde instead of formaldehyde was used due to its synthetic feasibility. The reference compounds **20Me** were obtained by *O*-methylation of **20H**. Detailed synthetic procedures and compound characterization data are supplied as Supporting Information.

Scheme 1. Synthesis of the *m*-DMABDIs



The X-ray crystal structures were determined for *m*-DMABDI, **10H**, and **20H**. The expected intramolecular H-bond OH••••N=C is observed for **20H**, but the hydroxyl group in **10H** is H-bonded to the imino nitrogen of the neighboring molecule (Figure S2). The benzylideneimidazolinone moiety is nearly coplanar and the dimethylamino (DMA) group is in a syn orientation to the carbonyl group (as shown in Figure 1) for all three cases. The discrepancy in the DMA orientation and/or the H-bonding mode between the DFT-optimized and X-ray crystal structures could be attributed to the larger basicity<sup>12</sup> of the imino nitrogen vs the carbonyl oxygen and to the crystal packing effect.

The absorption spectra of the *m*-DMABDIs in hexane are shown in Figure 2. The spectral maximum ( $\lambda_{abs}$ ) is near 350 nm, and a long-wavelength shoulder with noticeable absorbance up to 480 nm is present for all cases. The peak maximum is of little dependence on the solvent polarity; the magnitude of the solvatochromic shift from hexane to MeOH is 1–3 nm (Table S3). The difference of  $\lambda_{abs}$ between **10H** and **10Me** and between **20H** and **20Me** is little or none, revealing a weak H-bonding effect on  $\lambda_{abs}$ .

<sup>(8)</sup> Yang, J.-S.; Huang, G.-J.; Liu, Y.-H.; Peng, S.-M. Chem. Commun. 2008, 1344–1346.

<sup>(9)</sup> Yang, J.-S.; Liau, K.-L.; Li, C.-Y.; Chen, M.-Y. J. Am. Chem. Soc. 2007, 129, 13183–13192 and references cited therein.

<sup>(10)</sup> Kojima, S.; Ohkawa, H.; Hirano, T.; Maki, S.; Niwa, H.; Ohashi, M.; Inouye, S.; Tsuji, F. I. *Tetrahedron Lett.* **1998**, *39*, 5239–5242.

<sup>(11)</sup> Tanis, S. P.; Parker, T. T.; Colca, J. R.; Fisher, R. M.; Kletzein, R. F. J. Med. Chem. 1996, 39, 5053–5063.

<sup>(12)</sup> Dong, J.; Solntsev, K. M.; Tolbert, L. M. J. Am. Chem. Soc. 2006, 128, 12038–12039.

A similar situation was also reported for an intramolecularly H-bonded derivative of *p*-HBDI.<sup>13</sup>

Unlike the case of  $\lambda_{abs}$ , the fluorescence maximum ( $\lambda_f$ ) exhibits a large solvatochromic effect (e.g., a shift of 4190–4770 cm<sup>-1</sup> from hexane to MeCN, Figure S3 and Table 1), indicating the prominent charge-transfer character of the *m*-DMABDIs in the excited state. A spectrum of color from blue to red is observed for the fluorescence of *m*-DMABDI on going from hexane to MeCN (TOC graphic). The prominent solvatofluorochromism of *m*-DMABDI is reminiscent of the colorful mutants of GFP.<sup>14</sup> The solvatofluorochromic shift is slightly decreased for **10Me** and **20Me**. The  $\lambda_f$  values of **10H** and

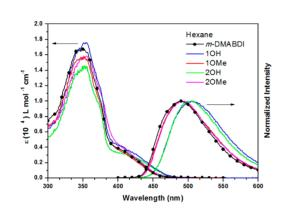


Figure 2. Absorption and fluorescence spectra of the *m*-DMAB-DIs in hexane.

**2OH** are at longer wavelengths relative to those of **1OMe** and **2OMe**, which is consistent with H-bonding interactions at the acceptor moiety of a donor-acceptor chromophore. The slightly larger difference in  $\lambda_f$  for **1OH** and **1OMe** (15–24 nm) compared to **2OH** and **2OMe** (10–16 nm) shows a larger electronic perturbation by H-bonding to the carbonyl oxygen than to the imino nitrogen.

The  $\Phi_f$  and the  $Z \rightarrow E$  isomerization quantum yield  $(\Phi_{ZE})$  of the *m*-DMABDIs in hexane, THF, and MeCN are reported in Table 1. The  $\Phi_f$  of the *m*-DMABDIs in hexane is in the range 0.37–0.46, which is larger than that of *m*-ABDI ( $\Phi_f = 0.34$  in hexane)<sup>8</sup> and the other unconstrained GFP-like chromophores in solutions.<sup>15</sup> As in the case of *m*-ABDI, the  $\Phi_f$  decreases as the solvent polarity increases, and the fluorescence is nearly quenched in MeOH ( $\Phi_f < 10^{-3}$ ). According to the one-bond-flip

model for the Z-E photoisomerization,<sup>16</sup> the quantum yield for the torsion of the exocyclic C=C bond is approximately equivalent to  $2\Phi_{ZF}$ , assuming that partitioning of the perpendicularly twisted intermediate to the Z and the Eisomers is equal. That  $\Phi_f + 2\Phi_{ZE} \approx 1.0$  for *m*-DMABDI, 10Me, and 20Me thus indicates that the excited-state deactivation is mainly due to fluorescence and the  $Z \rightarrow E$ isomerization and other internal conversion channels are unimportant. In contrast, it is  $\Phi_f + 2\Phi_{ZE} \ll 1.0$  for **10H** and **20H**. The decrease in  $\Phi_f$  and  $\Phi_{ZE}$  for the H-bonded and non-H-bonded couples (10H vs 10Me and 20H vs **20Me**) are 4-50% and 38-64%, respectively, and the difference is larger in more polar solvents. Evidently, the intramolecular H-bonding induces a new nonradiative decay channel that competes effectively with the fluorescence and Z, E-isomerization.

The site-dependent H-bonding effect is even more explicit with the comparison of radiative  $(k_r = \Phi_f/\tau_f)$  and nonradiative  $(k_{nr} = (1 - \Phi_f)/\tau_f)$  decay rate constants deduced from  $\Phi_f$  and the fluorescence lifetimes  $(\tau_f)$ . These data are shown in Table 1, and the uncertainty is 10% of the values. All the fluorescence decay profiles can be well fit

Table 1. Photophysical and Photochemical Data for the	
m-DMABDIs in Hexane (Hex), THF, and MeCN	

compd	solvent	$\begin{matrix} \lambda_f \\ (nm) \end{matrix}$	$\Phi_{\mathrm{f}}$ (%)			$k_{ m f} \ (10^8  { m s}^{-1})$	$\frac{k_{\rm nr}}{(10^8{\rm s}^{-1})}$		
m-DMABDI	Hex	492	46	21	22.5	0.20	0.24		
	THF	584	14	38	15.3	0.09	0.56		
	MeCN	643	<b>5</b>	53	8.6	0.06	1.11		
10H	Hex	506	43	n.d.	20.8	0.21	0.27		
	THF	585	12	26	12.1	0.10	0.73		
	MeCN	656	2	17	2.8	0.07	3.50		
10Me	Hex	491	45	n.d.	21.2	0.21	0.26		
	THF	563	13	42	14.7	0.09	0.59		
	MeCN	632	4	40	7.9	0.05	1.22		
2 <b>OH</b>	Hex	506	37	n.d.	18.9	0.20	0.33		
	THF	585	11	27	13.2	0.08	0.67		
	MeCN	642	3	16	5.2	0.06	1.87		
20Me	Hex	495	43	n.d.	22.4	0.19	0.25		
	THF	569	14	47	15.3	0.09	0.56		
	MeCN	632	6	44	7.7	0.08	1.22		

<sup>*a*</sup> For the purpose of solubility  $(10^{-3} \text{ M})$ , Hex and MeCN solutions contain 20% THF for the measurement of  $\Phi_{ZE}$ . Data are not determined (n.d.) in hexane because of poor solubility, even containing 20% THF. Excitation wavelength is 350 nm. <sup>*b*</sup> The  $\tau_{\rm f}$  was determined with excitation and emission around the spectral maxima.

with a single-exponential function. Unlike the subpicosecond fluorescence lifetime of *p*-HBDI,<sup>16</sup> the  $\tau_{\rm f}$  of **20Me** is as long as 22.4 ns in hexane, which is to our knowledge unprecedented for an unconstrained GFP-like chromophore.<sup>15,17</sup> The  $\tau_{\rm f}$  and  $k_{\rm f}$  decrease with increasing solvent polarity. This might indicate intensity borrowing<sup>18</sup> from the higher

<sup>(13) (</sup>a) Petersen, M. Å.; Riber, P.; Andersen, L. H.; Nielsen, M. B. *Synthesis* 2007, 23, 3635–3638. (b) Lincke, K.; Solling, T.; Andersen, L. H.; Klaerke, B.; Rahbek, D. B.; Rajput, J.; Oehlenschlaeger, C. B.; Petersen, M. A.; Nielsen, M. B. *Chem. Commun.* 2010, 46, 734–736.

<sup>(14) (</sup>a) Tsien, R. Y. Annu. Rev. Biochem. **1998**, 67, 509–544. (b) Shaner, N. C.; Patterson, G. H.; Davidson, M. W. J. Cell. Sci. **2007**, 120, 4247–4260.

<sup>(15) (</sup>a) Ivashkin, P. E.; Yampolsky, I. V.; Lukyanov, K. A. *Russ. J. Bioorg. Chem.* **2009**, *35*, 652–669. (b) Huang, G.-J.; Yang, J.-S. *Chem.*— *Asian J.* **2010**, *5*, 2075–2085. (c) Chuang, W.-T.; Hsieh, C.-C.; Lai, C.-H.; Lai, C.-H.; Shih, C.-W.; Chen, K.-Y.; Hung, W.-Y.; Hsu, Y.-H.; Chou, P.-T. *J. Org. Chem.* **2011**, *76*, 8189–8202. (d) Lee, J.-S.; Baldridge, A.; Feng, S.; SiQiang, Y.; Kim, Y. K.; Tolbert, L. M.; Chang, Y.-T. *ACS Comb. Sci.* **2011**, *13*, 32–38.

<sup>(16)</sup> Zimmer, M. Cis-trans Isomerization in Biochemistry; Dugave, C., Ed.; Wiley-VCH: Weinheim, Germany, 2006; p 77.

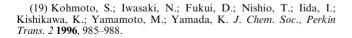
<sup>(17)</sup> Tolbert, L. M.; Baldridge, A.; Kowalik, J.; Solntsev, K. M. Acc. Chem. Res. 2012, 45, 171–181 and references cited therein.

<sup>(18)</sup> Bixon, M.; Jortner, J.; Verhoeven, J. W. J. Am. Chem. Soc. 1994, 116, 7349–7355.

excited state of the more allowed transition (Figure 2). In more polar solvents, the energetic separation between the fluorescing and the higher excited state is larger, and thus the intensity borrowing becomes lower. The natural fluorescence rate constant  $(k_f)$  of all five compounds in the same solvent is equivalent within experimental uncertainty, and thus the difference in  $k_{\rm f}$  between **10H** and **10Me** and that between 20H and 20Me is negligible. In contrast, the difference in  $k_{\rm nr}$  ( $\Delta k_{\rm nr}$ ) for the H-bonded vs non-H-bonded couple is substantial and solvent-dependent (Figure 3a). The  $\Delta k_{nr}$  is small  $((1-8) \times 10^6 \text{ s}^{-1})$  in hexane but significant  $((0.7-2.3) \times$  $10^8 \text{ s}^{-1}$ ) in MeCN for both H-bonding modes. The  $\Delta k_{nr}$  can be attributed to the rate constant of nonradiative decay induced by the intramolecular H-bond ( $k_{\rm HB} = \Delta k_{\rm nr}$ ). Although the DFT calculations suggest a more stable H-bonded state for **2OH** vs **1OH**, the  $k_{\rm HB}$  is 3.4-fold larger for 10H vs 20H in MeCN. Evidently, the H-bonding to the carbonyl oxygen is more impactful than that to the imino nitrogen on the excited-state quenching. As indicated by the  $\lambda_{\rm f}$  of **1OH** vs **2OH**, which is the same in hexane but larger in MeCN, the larger H-bonding effect in 10H results from stronger H-bonding interactions associated with the carbonyl vs the imino group in the electronically excited state.

The solvent effect on  $k_{\rm HB}$  provides insight to the nature of the H-bond-induced decay channel. In principle, the intramolecular H-bond is more favorable in less polar solvents.<sup>19</sup> A larger H-bonded population is thus expected for **10H** and **20H** in hexane than in MeCN. However, the  $k_{\rm HB}$  is much smaller in hexane vs MeCN, which indicates that the quenching of the excited state is not simply due to internal conversion. An occurrence of excited-state proton transfer (ESPT) from MeOH to the carbonyl oxygen or the imino nitrogen that results in a polar zwitterion might account for the larger  $k_{\rm HB}$  in more polar solvents due to better solvation.

The effect of intermolecular H-bonding on fluorescence quenching was also investigated with MeOH titration of *m*-DMABDI in MeCN (Figure 3b). Figure 3c shows the  $log(\Phi_{f0}/\Phi_f - 1)$  vs log[MeOH] plot, where  $\Phi_{f0}$  and  $\Phi_f$  correspond to the fluorescence quantum yield in the absence and presence of MeOH. The slope  $1.02 \pm 0.03$  indicates that the fluorescence quenching results from a 1:1 complex of *m*-DMABDI and MeOH.<sup>4</sup> According to the slope  $(3.35 \pm 0.07 \text{ M}^{-1})$  of the Stern–Volmer plot (Figure 3d) and fluorescent lifetime (8.6 ns) in MeCN, the calculated quenching constant is  $3.6 \times 10^8 \text{ M}^{-1} \text{ s}^{-1}$ . This value is nearly 100 times smaller than the diffusional rate constant in MeCN ( $2.3 \times 10^{10} \text{ M}^{-1} \text{ s}^{-1}$ ),<sup>3a</sup> which



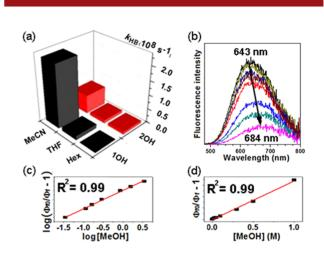


**Figure 3.** (a) Comparison of  $k_{\rm HB}$  in different solvents and H-bonding modes; (b) MeOH-induced fluorescence quenching for *m*-DMABDI in MeCN ([MeOH] = 0.0–1.0 M), and the corresponding (c) plot of log( $\Phi_{\rm f0}/\Phi_{\rm f}$  – 1) against log[MeOH] and (d) Stern–Volmer plot.

indicates that a significant barrier exists in the quenching process or it is static quenching due to ground state complexation. The low  $\Phi_{\rm f}$  ( $< 10^{-3}$ ) in neat MeOH suggests a  $k_{\rm HB}$  value larger than  $1 \times 10^9 \, {\rm s}^{-1}$ , provided that all of the substrate forms the complex and the  $k_{\rm f}$  is on the same order as that in MeCN. A smaller  $k_{\rm HB}$  for **10H** in MeCN (2.3 ×  $10^8 \, {\rm s}^{-1}$ ) vs *m*-DMABDI in MeOH ( $> 1 \times 10^9 \, {\rm s}^{-1}$ ) reflects the low population of the optimal H-bonded form of **10H**.

In summary, the H-bonding to the carbonyl oxygen of the *m*-DMABDIs plays a more important role than that to the imino nitrogen in deactivating the excited state. The intriguing dependence of fluorescence properties on solvent polarity and proticity for the *m*-DMABDIs and their analogs might prove of value as fluorescent probes for siteselective fluorescence imaging of biological systems.

Acknowledgment. We thank the National Science Council of Taiwan and National Taiwan University for financial support. The computing time granted by the Computing Center of NTU is acknowledged.

**Supporting Information Available.** Detailed experimental methods and synthesis, fluorescence spectra, X-ray crystal and DFT-optimized structures, table of maxima of UV/vis absorption ( $\lambda_{abs}$ ) and fluorescence ( $\lambda_f$ ), and CIF file for the *m*-DMABDIs. This material is available free of charge via the Internet at http://pubs.acs.org.

The authors declare no competing financial interest.